



EFFECTS OF ELECTROCHEMICAL AND THERMAL OXIDATION ON THE BEHAVIOUR OF SOME BIOMATERIALS IN SIMULATED BODY FLUIDS

Julia C. MIRZA ROSCA,^a Mihai V. POPA,^b Ecaterina VASILESCU,^b Paula DROB,^b
Cora VASILESCU^{b*} and Silviu I. DROB^b

^a Las Palmas de Gran Canaria University, Mechanical Engineering Department, Despacho 11, 35017 Tafira, Spain

^b Institute of Physical Chemistry "Ilie Murgulescu", Spl. Independentei 202, 060021 Bucharest, Roumania

Received February 22, 2010

The effects of electrochemical and thermal oxidation on the behaviour of Ti and its implant alloys Ti-5Al-4V and Ti-6Al-4Fe in Ringer solution are investigated in this paper, using microscopic observations, microhardness measurements, electrochemical impedance spectroscopy (EIS) and long-term monitoring of the open circuit potentials. The microhardness values increased with increasing load, showing the existence of a porous layer; no differences between the applied treatments were observed, revealing the same composition and average depth of the oxide layers. EIS spectra exhibited a two-step process, namely an oxide with two layers: a porous, outer oxide and a barrier inner oxide; some differences appeared in time, due to the apatite nucleation. Statistical analysis of the open circuit potentials for bare Ti and Ti-5Al-4V and Ti-6Al-4Fe alloys supplied histograms, scatter diagrams, regression equations and determination coefficients. A good percent of credibility it resulted and a prognosis can be made.

INTRODUCTION

Titanium and its alloys have been widely used as implants due to their good corrosion resistance, mechanical properties (high fracture toughness and load-bearing resistance) and biocompatibility.¹⁻⁶ But, the long-term stability and bone fixation of these materials are the important factors for their functionality.^{7,8} Hydroxyapatite (HA) coatings have been shown to improve the bone bonding⁹ and the barrier effect on the metal ion release.¹⁰ The presence of the long-term stable HA layer with a thickness of about 150 μm ⁸ can ensure a permanent bond between implant and bone and can guarantee the implant stability. Another advantages of HA coating include: an optimized bone bridging capacity in the case of gaps at the interface and the absence of fibrous capsules of connective tissue surrounding the implant; fast bone apposition rates through preferential adsorption of proteins; bonding osteogenesis providing a continuous and strong interface between implant and tissue that is able to transmit not only compressive but also tensile and shear stresses; accelerated healing

compared to implants without an osteoconductive coating; reduced release of ions, minimizing the risk of cytotoxic response.^{8,11}

It was demonstrated that titanium and its alloys with their stable titanium dioxide (in two allotropic forms; rutile and anatase) are most effective for apatite nucleation.¹²⁻¹⁴ Anodic oxidation is a superior method to obtain rough, porous oxide surfaces^{15,16} proper to develop the apatite-forming ability.

The anodic oxidation can be made in alkaline (sodium hydroxide) or acid (sulphuric acid) solutions.¹⁷⁻²² After the anodic oxidation and the subsequent heat treatment, the ability of the titanium metals to form apatite in body fluids it is increased and accelerated. So, it is promoted the bounding of the implant to the surrounding bone.

The anodic oxide films were formed on titanium and its implant alloys Ti-5Al-4V and Ti-6Al-4Fe by electrochemical treatment in 3M sulfuric acid solution and followed by a heat treatment. The effects of these electrochemical and heat treatments on the biomaterials behaviour in Ringer solution were investigated in this paper.

* Corresponding author: cvasilescu@chimfiz.icf.ro

EXPERIMENTAL

The composition of titanium and its Ti-5Al-4V, Ti-6Al-4Fe alloys is given in another paper.²³ Anodic oxide films on titanium and its implant alloys were prepared by electrochemical treatment in 3M sulphuric acid solution at 60 V for 1 minute, followed by a thermal treatment consisting of heating at 500°C for 24 hours and then cooled in water. Three types of samples were used: with electrochemical treatment (E); with heat treatment (H); with electrochemical and heat treatment (EH).

The effects of the electrochemical and heat treatments on the biomaterials behaviour were determined by: microscopic observations, microhardness measurements, electrochemical impedance spectroscopy (EIS) and by long-term monitoring of the open circuit potentials.

The sample surface was observed using an Optical Microscope.

The microhardness was measured by means of an indentation test (Remet HX-1000 Microhardness Tester) on the sample (discs) surfaces, applied tangentially to the surface with Vickers indenter, at every 0.5 mm along the diameter of the sample. Loads of 10, 25, 50 and 200 grams and time of 15 sec. were used. The average value for each sample, expressed as Hardness Vickers degree (HV) was calculated; based on this average value, the corresponding depth was calculated:

$$d = \sqrt{\frac{1.854 P}{49 HV}} \quad (1)$$

where: d = depth in mm; P – load in Kg; HV = Vickers microhardness.

Electrochemical impedance spectra were obtained at open circuit potential using a PAR 263A potentiostat connected with a PAR 5210 lock-in amplifier. The amplitude of the AC potential was 10 mV and single sine wave measurements at frequencies between 10^{-1} and 10^5 Hz were performed for each sample.

Open circuit potentials were monitored (long-term, 25000 exposure hours) in Ringer solution of different pH values (6.98, 4.35, 2.5, the acid pH was obtained by HCl addition) for titanium, Ti5Al-4V and Ti-6Al-4Fe alloys but without treatment, with the purpose to compare the behaviour of the uncovered biomaterials with the covered biomaterials.

All measurements were performed at 37°C temperature in Ringer solution of composition (g/L): NaCl –6.8; KCl –0.4; CaCl₂ –0.2; MgSO₄·7H₂O –0.2048; NaH₂PO₄·H₂O –0.143; NaHCO₃ –2.2; glucose–1.

A conventional three electrode electrochemical cell with a Pt grid as counter electrode and saturated calomel electrode (SCE) as reference electrode was used.

RESULTS AND DISCUSSION

Effects of oxidation treatments on the biomaterial behaviour by microscopic observation

A wide range of iridescent oxide colors on the surfaces of Ti and its alloys can be obtained by

anodic oxidation or/and heat treatment.^{1,24} The colors vary from yellow to red, purple bronze, etc. Colors depend on the oxide thickness, applied voltage and temperature of heat treatments. It was demonstrated^{18,25} that porous titanium dioxide (TiO₂) in anatase and rutile forms were obtained by anodic oxidation in sulphuric acid solution.

In our experiments, the initial, similar (yellow) colors were obtained both for Ti and its alloys, denoting the same composition and structure of the anodic films (Fig. 1a). After short-term exposure (about 300 hours) in Ringer solution, the colors changed to brown (Fig. 1b), denoting a change of the anodic layer composition or growth due to the apatite nucleation. This fact can be explained by the apatite formation: hydroxyl ions (OH⁻) from solution are adsorbed on the surface and lead to a negatively charge surface; this negative charge absorbs Ca²⁺ ions from Ringer solution and then, these positive calcium ions attract phosphate ions (PO₄³⁻) and form nucleation sites for apatite and facilitate the apatite deposition.^{17,18}

Effects of oxidation treatments on the biomaterial behaviour by Vickers microhardness measurements

From Table 1, it can be observed that, the microhardness increases with increasing load, showing the existence of a porous layer on the surface. Also, differences between samples with or without electrochemical treatment, or with and without heat treatment were not observed thus, pointing out the fact that the passive films have the same composition in all studied conditions. It was demonstrated^{16,25} that the porous anatase form of titanium dioxide is formed by treatment with sulphuric acid solution. This micro-porous structure is necessary for apatite formation; specific structural arrangement of anatase is effective in inducing apatite nucleation.^{26,27}

The average depth of the anodic oxide films determined by microhardness measurements vary about from 1 μm to 6 μm; these values are in agreement with those obtained by another authors.¹⁷

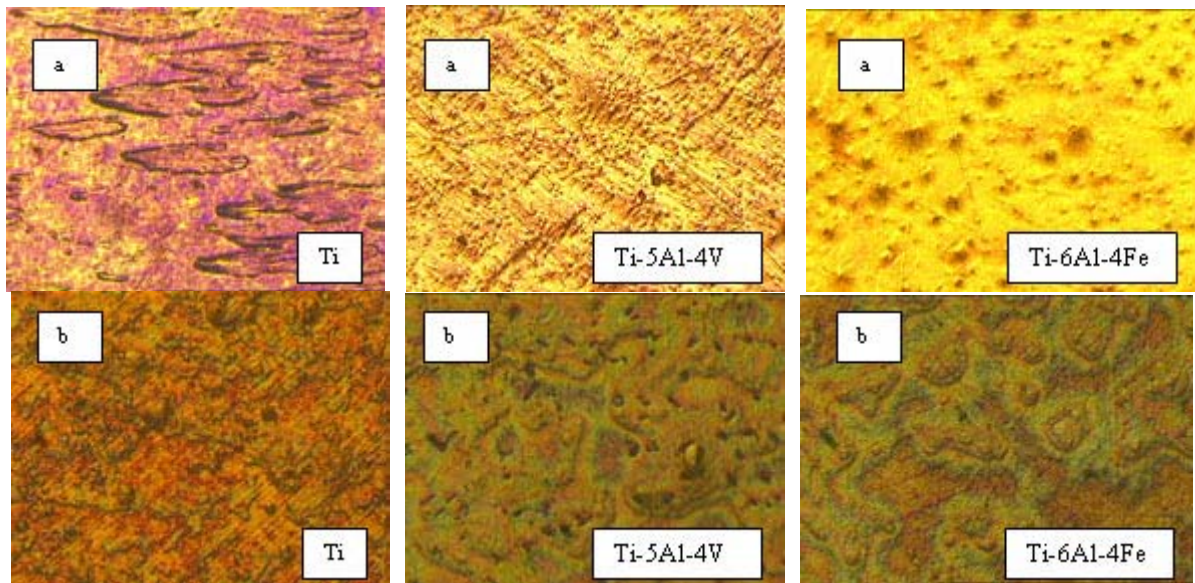


Fig. 1 – Aspects of samples before (a) and after 300 exposure hours (b) in Ringer solution.

Table 1

Microhardness and depth of anodic oxide films

Sample	Treatment	Load (g)	Hardness (HV)	Depth (μm)
Ti	E	10	155	1.56
		25	207	2.14
		50	223	2.91
		200	231	6.31
	H	10	189	1.41
		25	218	2.08
		50	215	2.97
		200	186	6.38
	EH	10	140	1.64
		25	180	2.29
		50	180	3.25
		200	182	6.45
Ti-5Al-4V	E	10	301	1.12
		25	373	1.59
		50	397	2.18
		200	422	4.23
	H	10	309	1.11
		25	414	1.51
		50	485	1.98
		200	420	4.24
	EH	10	287	1.14
		25	378	1.58
		50	401	2.17
		200	387	4.42
Ti-6Al-4Fe	E	10	285	1.15
		25	321	1.71
		50	360	2.29
		200	361	4.57
	H	10	232	1.28
		25	296	1.79
		50	305	2.49
		200	299	5.03
	EH	10	294	1.13
		25	322	1.71
		50	338	2.36
		200	350	4.65

Effects of oxidation treatments on the biomaterial behaviour by EIS

For electrochemical and heat treated titanium (Fig. 2), Bode plots for E type samples exhibited a two-step process or a system with two time constants, indicating an oxide with two layers, i. e. a porous outer oxide and a barrier inner oxide. This fact is confirmed by the phase angle almost -80° , typical for barrier oxide layer and another phase angle closed to -50° attributed to the porous layer

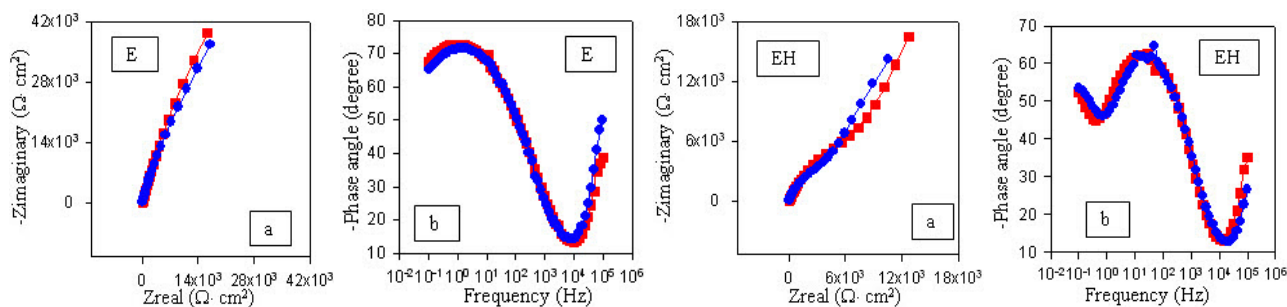


Fig. 2 – Nyquist (a) and Bode (b) plots for electrochemical (E) and heat (EH) treated Ti in Ringer solution after: -■- 3 days and -●- 7 days.

For Ti-5Al-4V alloy, the existence of two processes is clearly shown both for sample of E type and for EH type (Fig. 3), namely, a structure with two layers: a typical thin passive, barrier oxide (phase angle at about -80° for E type and at about -75° for EH type) and a porous another

(phase angle at about -50° for E type and at about -45° for EH type). With the increase of the exposure time, the values of the phase angle (from Bode plots) decreased and the linear part (from Nyquist plots) accentuated because of the porous apatite formation.

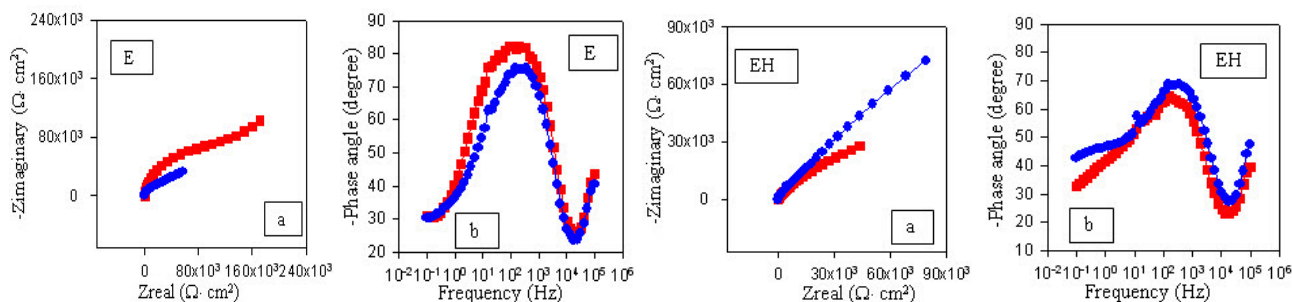


Fig. 3 – Nyquist (a) and Bode (b) plots for electrochemical (E) and heat (EH) treated Ti-5Al-4V alloy in Ringer solution after: -■- 3 days and -●- 7 days.

The same results were obtained for Ti-6Al-4Fe alloy (Fig. 4). Bode plots present two phase angles for a structure with two layers: for E type samples, the angles have values of about -80° for barrier layer and -40° for porous layer; for EH type samples, the compact layer is characterized by a phase angle of -75° and the porous layer is

represented by a phase angle of -45° . Nyquist plots show a depressed semicircle and a diffusion tail, confirming a bi-layered film. These facts attest that the anodic oxide films on surface have the same composition and structure both for titanium and its alloys.

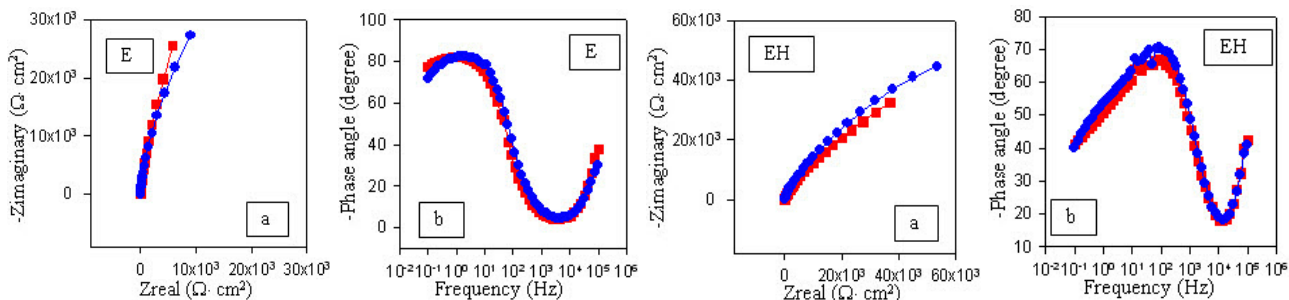


Fig. 4 – Nyquist (a) and Bode (b) plots for electrochemical (E) and heat (EH) treated Ti-6Al-4Fe alloy in Ringer solution after: -■- 3 days and -●- 7 days.

Statistical analysis of the open circuit potentials for bare Ti and Ti-5Al-4V and Ti-6Al-4Fe alloys

Open circuit potentials for bare Ti and Ti-5Al-4V and Ti-6Al-4Fe alloys were monitored for 25000 h in Ringer solutions of different pH values (6.98; 4.35; 2.5), simulating extreme functional conditions of an implant. For the characterization of the long-term behaviour of these biomaterials, the biostatistics was used.

Biostatistical analysis³² by Medcalc program represents the application of mathematics to biological phenomenon for to determine: histograms that show the frequency and distribution of the open circuit potential (E_{oc}) values; scatter diagrams of E_{oc} ; regression equations that describe E_{oc} – time relation and which can be used for to predict the E_{oc} values for

longer time than the experimental one; determination coefficients (D) for regression equations (values from 0.7 to 1.0 provide a high credibility level of the prognosis).

From histograms (Fig. 5-7) can be observed that at pH = 6.98 (Fig. 5), the main distribution of E_{oc} values is represented by electropositive potentials which are placed around -50 mV for Ti, around -150 mV for Ti-5Al-4V alloy and around -250 mV ÷ -100 mV for Ti-6Al-4Fe alloy (Table 2); all E_{oc} values are placed in the passive potential range of Ti, Al, V, Fe on the Pourbaix diagrams,³³ showing a very stable passive state. Comparing these three biomaterials it resulted that the alloys present a little more active open circuit potentials than Ti. But, all values are situated in the same passive domain, providing a good stability.

Table 2

Distribution of E_{oc} values in Ringer solutions from histograms

Biomaterial	E_{oc} (mV) values at:		
	pH = 6.98	pH = 4.35	pH = 2.5
Ti	-50	-350 ÷ -100	-300 ÷ -50
Ti-5Al-4V	-150	-400 ÷ -300	-400 ÷ -250
Ti-6Al-4Fe	-250 ÷ -100	-300 ÷ -200	-350 ÷ -300

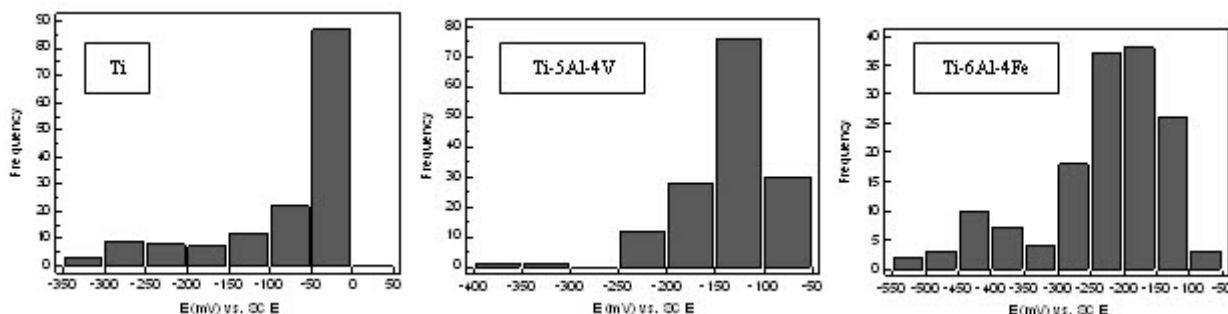


Fig. 5 – Histograms obtained in Ringer solution of pH = 6.98.

At pH = 4.35 (Fig. 6), majority values of E_{oc} are distributed around slight more electronegative values than at neutral pH = 6.98 (Table 2) and are

placed in the passive potential range³³ of Ti and Al, indicating some processes of dissolution and repassivation.²³

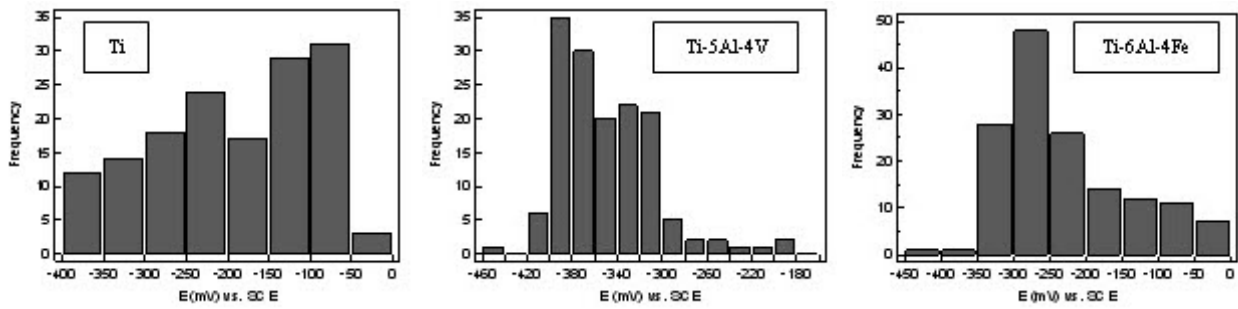


Fig. 6 – Histograms obtained in Ringer solution of pH = 4.35.

At very acid pH value of 2.5 (Fig. 7), the histograms show that the highest frequency of the open circuit potential distribution appeared at more electronegative values (Table 2) due to the fact that

the only Ti is placed in the passive state, the other alloying elements being in the active state,³³ therefore, at this pH value, Ti-5Al-4V and Ti-6Al-4Fe alloys are not stable.

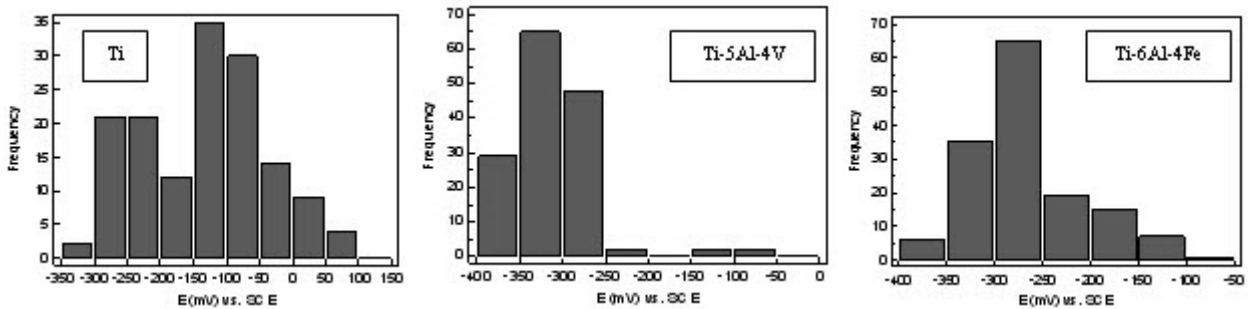


Fig. 7 – Histograms obtained in Ringer solution of pH = 2.5.

No apatite nucleation processes were observed.

Scatter diagrams (Fig. 8-10) were treated by regression procedure and the regression equations (polynomial equations) and determination coefficients (D) were obtained (Table 3). The values of the determination coefficients vary around 0.6 – 0.9 values, revealing a good percent

of credibility. So, it is possible to estimate the values of E_{oc} for longer time periods. But, in bioliquids, such prediction needs more precautions than in other cases, taking into account the fact that the human body is very complex and unexpected phenomenon could take place any time.

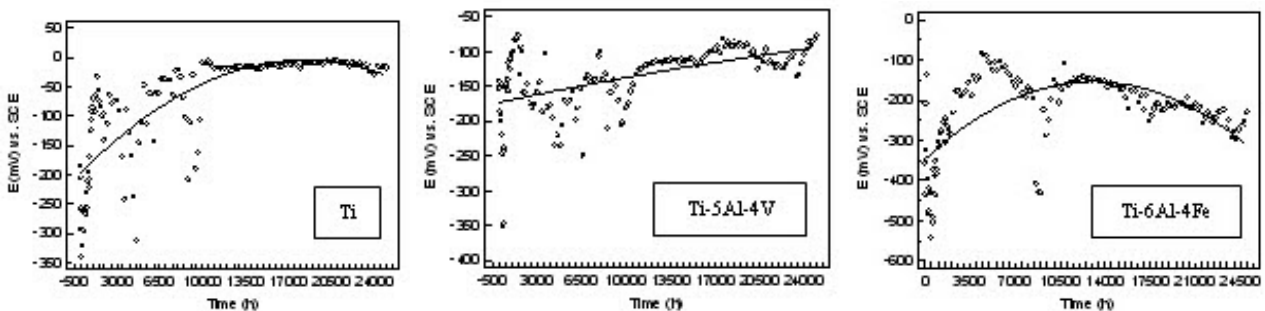


Fig. 8 – Scatter diagrams obtained in Ringer solution of pH = 6.98.

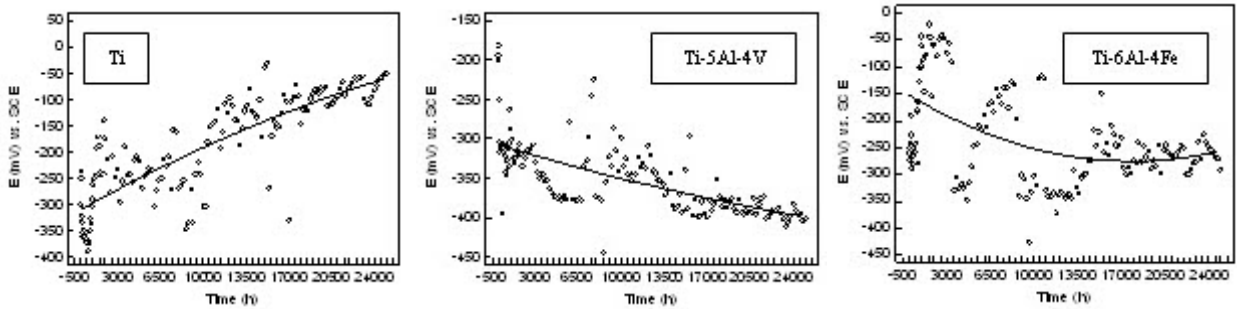


Fig. 9 – Scatter diagrams obtained in Ringer solution of pH = 4.35.

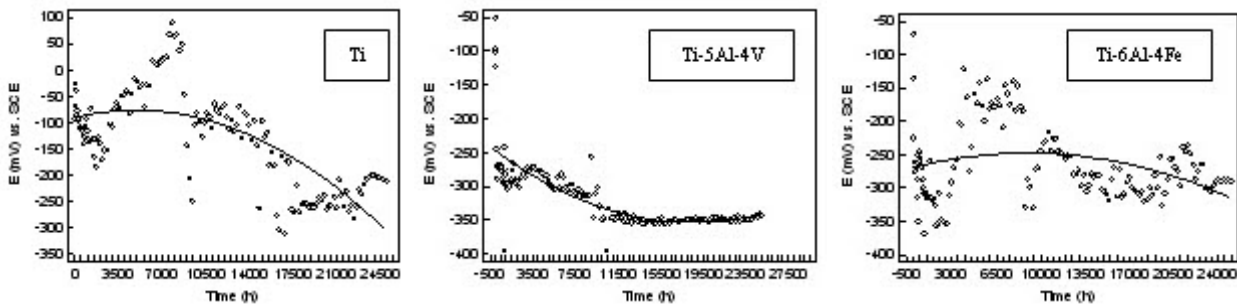


Fig. 10 – Scatter diagrams obtained in Ringer solution of pH = 2.5.

Table 3

Regression equations and determination coefficients (D) in Ringer solutions of different pH values

pH	Biomaterial	Regression equation	D
6.98	Ti	$y = -197.8037 + 0.02118 x + -0.0000005788 x^2$	0.64
	Ti-5Al-4V	$y = -172.1991 + 0.003787 x + -0.00000002478 x^2$	0.69
	Ti-6Al-4Fe	$y = -345.6854 + 0.02928 x + -0.000001118 x^2$	0.63
4.35	Ti	$y = -309.0765 + 0.01295 x + -0.0000001190 x^2$	0.69
	Ti-5Al-4V	$y = -307.5506 + -0.004713 x + 0.00000004179 x^2$	0.65
	Ti-6Al-4Fe	$y = -153.6788 + -0.01368 x + 0.0000003837 x^2$	0.64
2.5	Ti	$y = -89.7664 + 0.005427 x + -0.0000005637 x^2$	0.52
	Ti-5Al-4V	$y = -247.5973 + -0.01149 x + 0.0000003117 x^2$	0.68
	Ti-6Al-4Fe	$y = -268.4680 + 0.004655 x + -0.0000002608 x^2$	0.59

CONCLUSSIONS

Initial, similar (yellow) colors were obtained both for Ti and its alloys by electrochemical and thermal treatments; after 3000 exposure hours, the colors changed to brown for all samples, denoting the same composition and structure of the obtained anodic films.

The microhardness values increased with increasing load, showing the existence of a porous layer; no differences between the applied treatments were observed, revealing the same composition and average depth of the oxide layers.

EIS spectra exhibited a two-step process, namely an oxide with two layers: a porous, outer oxide and a barrier inner oxide; some differences appeared in time, due to the apatite nucleation.

Statistical analysis of the open circuit potentials for bare Ti and Ti-5Al-4V and Ti-6Al-4Fe alloys supplied histograms, scatter diagrams, regression equations and determination coefficients. A good percent of credibility it resulted and a prognosis can be made.

Acknowledgement. This work was supported by CNCSIS – UEFISCSU, project number PNII – IDEI code 248/2010.

REFERENCES

1. M. T. Pham, H. Reuther, W. Matz, R. Mueller, G. Steiner, S. Oswald and I. Zyganov, *J. Mater. Sci. Mater. M.*, **2000**, *11*, 383-391.
2. B. Feng, J. Y. Chen, S. K. Qi, L. H. Zhao and X. D. Zhang, *J. Mater. Sci.*, **2002**, *13*, 457-464.

3. A. Banu, O. Radovici and M. Marcu, *Rev. Roum. Chim.*, **2008**, *53*, 947-953.
4. V. Branzoi, F. Golgovici, L. Pilan, F. Branzoi and C. Anghel, *Rev. Roum. Chim.*, **2005**, *50*, 1013-1018.
5. A. Banu, M. Marcu and O. Radovici, *Rev. Roum. Chim.*, **2008**, *53*, 941-945.
6. D. C. Momete, E. Verne, C. Vitale Brovarone and D. S. Vasilescu, *Rev. Roum. Chim.*, **2006**, *51*, 47-52.
7. S. Fujibayashi, T. Nakamura, S. Nishiguchi, J. Tamura, M. Uchida, H-M. Kim and T. Kakubo, *J. Biomed. Mater. Res.*, **2001**, *56*, 562-570.
8. R. B. Heimann, N. Schurmann and R. T. Muller, *J. Mater. Sci. Mater. M.*, **2004**, *15*, 1045-1052.
9. M. Gotlander and T. Albrektsson, *Int. J. Oral Maxillofac. Jmp.*, **1991**, *6*, 339-345.
10. M. Wei, H. M. Kim, T. Kokubo and J. H. Evans, *Mat. Sci. Eng.C-Bio. S.*, **2002**, *20*, 125-134.
11. H. Caulier, J. P. C. M. Van der Waerden, J. G. C. Wolke, W. Kalk, I. Naert and A. Jansen, in "Materials in Clinical Applications", P. Vincenzini ed., pub. Techna Srl., 1995, p. 477-550.
12. D. Velten, V. Bichl, F. Anvertin, B. Valeske, W. Possart and J. Bume, *J. Biomed. Mater. Res.*, **2002**, *59*, 18-28.
13. M. Wei, M. Uchida, H. M. Kim, T. Kokubo and T. Nakamura, *Biomaterials*, **2002**, *23*, 167-172.
14. J. Marsh and D. Gorse, *Electrochim. Acta*, **1998**, *43*, 659-670.
15. H. Ishizawa and M. Ogino, *J. Biomed. Mater. Res.*, **1995**, *29*, 65-72.
16. J. R. Birch and T. D. Burleigh, *Corrosion*, **2000**, *56I*, 1233-1241.
17. X. X. Wang, W. Yan, S. Hayakawa, K. Tsuru and A. Osaka, *Biomaterials*, **2003**, *24*, 4631-4637.
18. B. Yang, M. Uchida, H. M. Kim, X. Zhang and T. Kakubo, *Biomaterials*, **2004**, *25*, 1003-1010.
19. B. Liang, S. Fujibayashi, M. Neo, J. Tamura, H. M. Kim, M. Uchida, T. Kakubo and T. Nakamura, *Biomaterials*, **2003**, *24*, 4959-4966.
20. R. Godley, D. Starosvesky and I. Gotman, *J. Mater. Sci. Mater. M.*, **2004**, *15*, 1073-1077.
21. V. Raghvan, *J. Phase Equilib.*, **2002**, *23*, 182-189.
22. X. Lu, Y. Lang and L. T. Wang, *J. Mater. Sci.*, **2004**, *39*, 6809-6811.
23. M. V. Popa, I. Demetrescu, E. Vasilescu, P. Drob, A. Santana Lopez, J. Mirza Rosca, C. Vasilescu, D. Ionita, *Electrochim. Acta*, **2004**, *49*, 2113-2117.
24. E. Gual, *J. Chem. Educ.*, **1993**, *70*, 176-181.
25. J. M. Wu, S. Hayakawa, K. Tsuru and A. Osaka, *Thin Solid Films*, **2002**, *414*, 275-280.
26. J. M. Wu, S. Hayakawa, K. Tsuru and A. Osaka, *J. Am. Soc.*, **2004**, *87*, 1635-1642.
27. M. Uchida, H. M. Kim, T. Kokubo, S. Fujivayashi and T. Nakamura, *J. Biomed. Mater. Res.*, **2003**, *64*, 164-170.
28. R. Venugopalan, J. J. Weimer, M. A. George and L. C. Lucas, *Biomaterials*, **2000**, *21*, 1669-1677.
29. J. E. G. Gonzalez and J. C. Mirza Rosca, *J. Electroanal. Chem.*, **1999**, *109*, 4711-4721.
30. E. Vasilescu, P. Drob, D. Raducanu, I. Cincea, D. Mareci, J. M. Calderon Moreno, M. Popa, C. Vasilescu and J. C. Mirza Rosca, *Corros. Sci.*, **2009**, *51*, 2885-2896.
31. M. V. Popa, E. Vasilescu, P. Drob, I. Demetrescu, B. Popescu, D. Ionita and C. Vasilescu, *Mater. Corros.*, **2003**, *54I*, 215-219.
32. B. Rosner, "Fundamentals of Biostatistics", Boston, 1990, PWS-Kant., Boston Mass.
33. M. Pourbaix, "Atlas of Electrochemical Equilibria in Aqueous solutions", Houston, 1974, NACE.